Three-phase transformer representation using FEMM, and a methodology for air gap calculation

Conference Paper · October 2008

DOI: 10.1109/ICELMACH.2008.4799982 · Source: IEEE Xplore

3 authors:

E. Saraiva
Universidade Federal de Uberlândia (UFU)
30 PUBLICATIONS **73** CITATIONS
SEE PROFILE

Marcelo Lynce Ribeiro Chaves
Universidade Federal de Uberlândia (UFU)
57 PUBLICATIONS **191** CITATIONS
SEE PROFILE

José Roberto Camacho
Universidade Federal de Uberlândia (UFU)
167 PUBLICATIONS **333** CITATIONS
SEE PROFILE

Three-Phase Transformer Representation Using FEMM, and a Methodology for Air Gap Calculation

Elise Saraiva*, MSc; Marcelo L. R. Chaves, Dr.; José R. Camacho, PhD
School of Electrical Engineering, Universidade Federal de Uberlândia;
Av. João Naves de Ávila, 2121; Campos Santa Mônica; Uberlândia; Minas Gerais, Brazil
Tel: (34)-3239-4774, fax: (34)-3239-4704
*e-mail: elise.saraiva@yahoo.com.br

***Abstract*- This work deals with the representation of three-phase and three-limb transformers in two dimensions using FEMM (Finite Element Methods on Magnetics). The transformer magnetization curve is obtained using the magnetization characterisitic for the silicon steel used when assembling the transfornmer core, associated to the air gaps inherent to the assembling process. A method for the calculation of the air gaps reluctance is presented and it is based on the transformer magnetic circuit and on the maximum value in each winding for the magnetization current waveform, such current is obtained through the no-load test. The magnetic flux distribution in the limb and yoke segments of the core are compared with design values and the effects of inherent airgaps in the magnetization current is analized. Through the use of post-processing procedures, the transformer leakage reactance is calculated and compared with values obtained through the experimental method. Therefore, one of the objectives, is to explain a method to insert some of the transformer assembling imperfections in the computer model.**

I. INTRODUCTION

The behavioral study of electrical machines, generically, is made through models based in the equivalent circuit [1]. Precision of results are reliant upon how the equivalent circuit parameters are obtained. Most of the time, such parameters are obtained through standard tests for each kind of machine, and they take in consideration that the machine is symmetrical.

The leakage reactance of a transformer and the core magnetization curve are essential for the model, mainly when the study is based on the magnetic flux distribution of the whole machine. In such cases, the effects of winding and core symmetry must be taken in consideration [2]. Therefore the computation of leakage reactance and the determination of magnetization curve through various analytical and numerical methods don't have the required precision, especially when it is a three-limb transformer core [3]. In this kind of transformer the magnitude of the magnetization current in each of the phases are not the same and generically the radial and axial dimensions of high and low voltage windings are different [4]. Added to this fact, it is difficult to make tests for the determination of the transformer magnetization curve in its higher saturation levels, as such the ones that happen during the transformer energization process.

In this paper is presented a technique for the representation of three-phase and three-limb transformers with the aid of FEMM [5], free-source software that is widely used by the academic community to simulate electromagnetic phenomena in a two-dimension environment.

The computation methodology is the finite elements method and it is structured in three stages: pre-processing, processing and post-processing [6]. The main characteristic of this technique here presented is the use of a silicon steel magnetization curve used in the core, associated to small air gaps, that comes from the assembling joints in the silicon steel sheets when mounting the core. The idea consists into the establishment of the possibility of modeling the existence of such air gaps due to the assembling and to distribute the effect along the transformer core. From such constraints, to build a magnetic circuit formed by magnetomotive sources and reluctances of silicon steel parts in the core, and the air gaps. Reluctances of silicon steel parts are obtained from the expected flux, magnetic characteristics of the silicon steel sheets and magnetic core geometrical dimensions. Reluctances associated to air gaps are related to the design peculiarities and core assembling aspects for each transformer. In such a way, those characteristics must be computed after the transformer assembling, taking as a basis the maximum absolute value in the magnetization current waveform in each winding, obtained from the no-load test. Depending upon the nature of the problem, the air gap reluctances can be associated in order to make the computation simpler and to reduce the computational effort.

The FEMM program does the transformer representation in two dimensions only, so it has some limitations for the representation of coils and limbs in cylindrical shapes along the third dimension (iron core depth), some adaptation is necessary in the geometric dimensions for the results to be in agreement with laboratory experiments.

II. TRANSFORMER CHARACTERISTICS

In this work will be used a transformer specially built for laboratory tests, with characteristics typical of a distribution transformer. This transformer has similar primary and secondary windings, being both low voltage windings, to make easier laboratory measurements. On the other hand, the assembling characteristics of such coils follow the typical standards for the low and high voltage windings of a distribution transformer. Table I presents other significant transformer characteristics.

978-1-4244-1736-0/08/$25.00 ©2008 IEEE

TABLE I
TRANSFORMER CHARACTERISTICS

Transformer power	15 kVA	
Voltage	Wind. ext. & int.	220 V
Connection type	Wind. ext. & int.	wye
Copper wire dimensions	Wind. ext. & int.	3.5x4.5 mm
Number of turns	Wind. ext. & int.	66
Aparent cross section area	limb	0.0049996 m^2
	yoke	0.0052826 m^2
Net cross section area	limb	0.0047496 m^2
	yoke	0.0050185 m^2
Width	limb	0.080 m
	yoke	0.066 m
Magnetic flux density	limb	1.55 Tesla
	yoke	1.44 Tesla
Impedance in percent	3.47 %	

Figure 1 shows the upper view of the transformer core and windings, Figure 2 shows de front view, and Figure 3 shows the B-H curve for the silicon steel sheet used in the assembling of the core (provided by ACESITA). Such figures show in detail some core and winding sizes, those dimensions will be of extreme importance for the transformer modeling using FEMM.

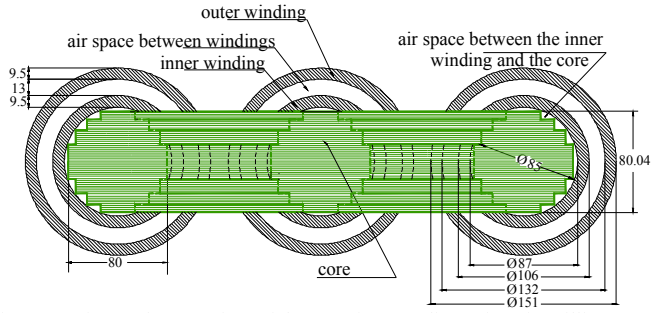

Fig. 1. An internal upper view of the transformer (dimensions in millimeters).

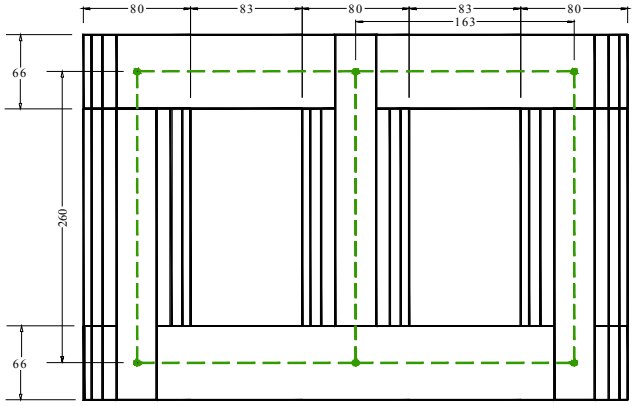

Fig. 2. Transformer core front view (dimensions in millimeters).

In Figures 1 and 2 can be observed that the limbs and the windings have the cylindrical shape, and this format along the third dimension can not be accurately represented in FEMM. Hence, some geometrical changes are necessary to keep the same area for the core and windings.

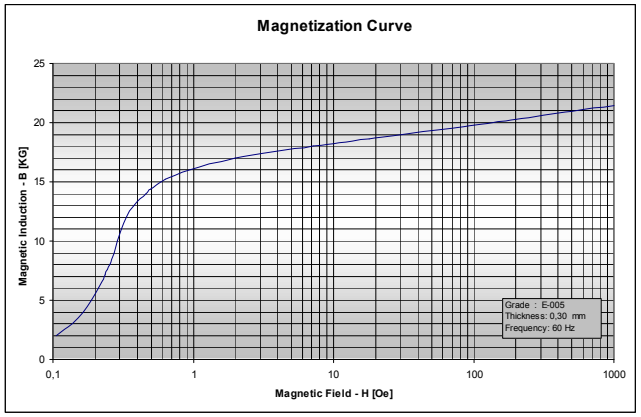

Fig. 3. Magnetization characteristic for the silicon steel sheets E005 provided by ACESITA.

In Table II can be seen the peak values for the magnetization currents in each of the three phases, obtained through the no-load test, with the wye, without earth, connection.

TABLE II
PEAK VALUE FOR THE MAGNETIZATION CURRENT

I_A [A]	I_B [A]	I_C [A]
2.34	1.54	2.34

III. TRANSFORMER MODELING USING FEMM

A. *Magnetic core considerations*

The FEMM program does electromagnetic simulations in two dimensions only, and is not suitable for the correct representation of the transformer limbs (three teeth cross) and windings (cylinder) in its original shape, due to the fact that all the geometric representation is made using horizontal and vertical dimensions for a given depth. In this case it is used as a depth the height of the pack of magnetic sheets from which the core is made, it is equivalent to 80.04 mm as shown in Figure 1.

Therefore, the limb magnetic section will be represented in the rectangular form with equivalent area. So, the width used for the limb will be 62.46 mm. This modification is made in such a way not to change the average length of the magnetic circuit.

Making such adjustments and inserting in FEMM all the necessary dimensions shown in Figure 2, as well as the magnetization curve for the iron core, taking in consideration the lamination fill factor as 0.95, a simulation is made taking in consideration the no-load transformer with normal excitation (at nominal voltage), at the instant where the current in phase A is at its peak value. In this simulation, currents at phases B and C were adjusted in such a way that the magnetic flux distribution imposed by the applied voltage is obtained. In this case the values used for the current in the simulation are presented in Table III.

TABLE III
CURRENT IN PHASES A, B AND C, USED IN THE SIMULATION

I_A [A]	I_B [A]	I_C [A]
2.340	1.122	1.218

The simulation result is shown in Figure 4, which presents the core magnetic flux distribution in the transformer. It can be verified that the values of magnetic flux density in the limb and yoke relatively to phase A are, respectively, 1.73 T and 1.64 T.

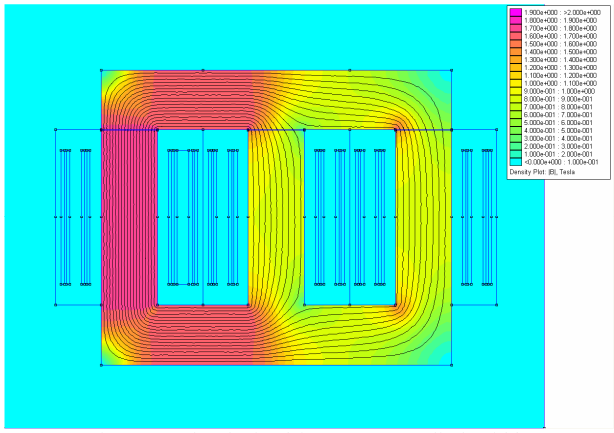

Fig. 4. Results obtained for a 62.46 mm limb width.

It can be observed that the values are not the expected, 1.55 T for the limb and 1.44 T for the yoke. Such discrepancy can be justified by the existence of small air gaps that take place during the core assembling. Such air gaps, in spite of being small, are significative in the composition of the necessary magnetomotive force for the magnetic flux, and they were responsible for the no-load current imposition.

B. Air gap insertion

For the insertion of air gaps in the model, it is necessary to know the size of them. However, this is data is not given by the manufacturer and is impossible to be measured. In this way, the option was to compute such values through calculations properly based, having as a basis the magnetization current peak value.

To carry out such computation it will be considered that the transformer is connected to a three-phase symmetrical voltage source, thus, the flux distribution relative to the instant in which the magnetic flux in the central limb reaches its peak value can be seen in Figure 5. The condition of symmetry for the voltage source imposes that when the flux assumes its peak value in one limb (central), the flux in the other two limbs will match the half of the value and in the opposite direction.

The air gaps that may be arising from the assembling of sheets can be seen in Figure 5, which are represented by its respective magnetic reluctances ($\Re_1$, $\Re_2$, $\Re_3$, $\Re_4$, $\Re_5$, $\Re_6$ e $\Re_7$). In this figure is observed the air gaps of superior and inferior yokes in the same side of the magnetic core, having as a reference the central limb, are always in series with the air gap of the external limb at the same side. This allows their association in a unique air gap. In this way, with the purpose of computation, it can be considered the magnetic core composed by three air gaps: the first relative to the left external limb and superior and inferior yokes at the left side denoted by ($\Re_e$), the second related to the central limb ($\Re_c$), and the third related to the right external limb and superior and inferior yokes at the right side ($\Re_d$).

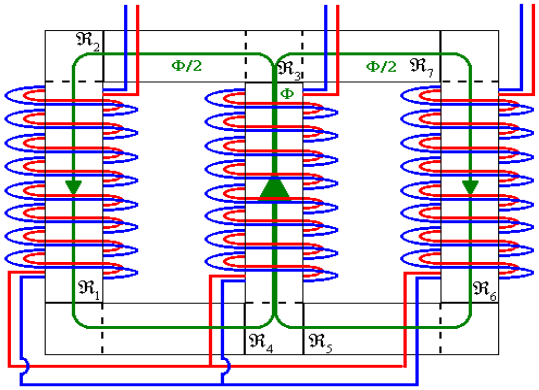

Fig. 5. Magnetic flux distribution for the no-load transformer, with the flux peak value at the central limb.

The air gaps can be all with different sizes since that their dimensions rely on specific details of the steel sheets cutting process and their assembling in the core composition. Such air gaps have direct influence in the transformer magnetization current in each phase; this is the reason why they are determined based in the values of such magnitudes.

The non-linearity, for the magnetic circuit, associated to the hysteresis cycle define the distorted waveform for the magnetization current, although, can be shown that the peak value for the magnetization current match the peak value for the magnetic flux in the same winding. However, the flux distribution shown in Figure 5 requires the peak value for the magnetization current at the central limb winding, but at the windings in the other two limbs, the condition of half of the flux peak doesn't imply in half of the peak value for the magnetization current. Other important issue to be taken into consideration is that the hysteresis cycle is not being taken in consideration by FEMM, consequently, the measured current waveform can not be the same used in the simulation. Hence, only the magnetization current peak values measured at the windings are used.

Different values of magnetic flux lead to different values of core reluctance. These values can be easily computed through the use the magnetic material B-H curve.

Considering I_A, I_B, e I_C, the transformer magnetization current peak values in the windings respectively of left external, center and right external limbs, a system of equations can be written for the magnetomotive forces considering the instants in which the magnetic flux has its peak value in each limb.

1) Condition 1: Maximum flux at the central limb.

Figure 6 pictures the transformer equivalent magnetic circuit at the instant which the flux reaches its peak value at the central limb (phase B). This situation has been depicted in

Figure 5 and the flux in the central limb is symmetrically split to the external limbs imposed by the voltage source.

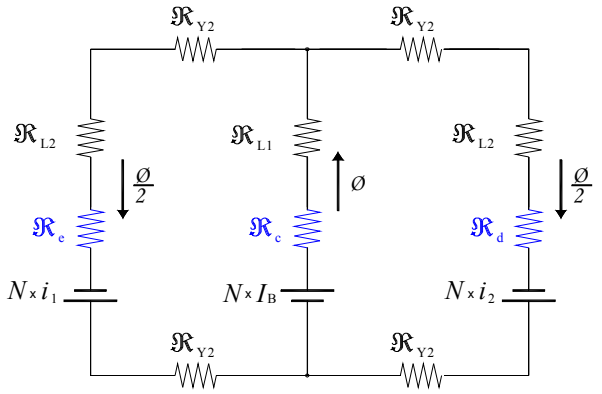

Fig. 6. Transformer equivalent magnetic circuit for the no-load condition, at the instant of maximum flux at the central limb.

Where:

- ϕ – Magnetic flux [Wb];
- N – Winding number of turns;
- $\Re_{L1}$ e $\Re_{Y1}$ – Limb and yoke reluctances for the flux peak value (ϕ) [H^{-1}];
- $\Re_{L2}$ e $\Re_{Y2}$ – Limb and yoke reluctances for the half of the flux peak value (ϕ/2) [H^{-1}];
- I_B – Transformer magnetization current peak value in the central limb winding [A];
- i_1 e i_2 – Instantaneous values for phases A and C currents, at the instant which the current at phase B is a maximum [A];
- $\Re_d$, $\Re_e$, $\Re_c$ – Right, left and center limb air gap reluctances, respectively [H^{-1}];

According Figure 6, and with the analysis of the closed circuit formed by the center and left limbs, it can be obtained the following equation:

$$N \times I_B + N \times i_1 = \Re_{L1} \times \phi + \Re_{L2} \times \frac{\phi}{2} + \\ + \Re_{Y2} \times \phi + \Re_e \times \frac{\phi}{2} + \Re_c \times \phi \quad (1)$$

With the knowledge that the current at phase B (I_B) is equivalent to the algebraic sum of currents in the other two phases (i_1 e i_2), condition imposed by the inexistence of a neutral connection, the following relationship is them true:

$$i_2 = I_B - i_1 \quad (2)$$

With the analysis of the closed circuit formed by the right and center limbs in Figure 6, it is obtained equation (3), in which the value of i_2 is replaced by equation (2).

$$2 \times N \times I_B - N \times i_1 = \Re_{L1} \times \phi + \Re_{L2} \times \frac{\phi}{2} + \Re_{Y2} \times \phi + \\ + \Re_c \times \phi + \Re_d \times \frac{\phi}{2} \quad (3)$$

Adding equations (1) and (3) the following equation is obtained:

$$3 \times N \times I_B = 2 \times \Re_{L1} \times \phi + \Re_{L2} \times \phi + 2 \times \Re_{Y2} \times \phi + \Re_e \times \frac{\phi}{2} + \\ + 2 \times \Re_c \times \phi + \Re_d \times \frac{\phi}{2} \quad (4)$$

2) Condition 2: Maximum flux at the left external limb.

With the same reasoning of *Condition 1*, only that now is considered that the flux reaches its maximum in the left external limb (phase A), them equation (5) is obtained.

$$3 \times N \times I_A = 2 \times \Re_{L1} \times \phi + \Re_{L2} \times \phi + 4 \times \Re_{Y1} \times \phi \\ + \Re_{Y2} \times \phi + 2 \times \Re_e \times \phi + \Re_c \times \frac{\phi}{2} + \Re_d \times \frac{\phi}{2} \quad (5)$$

3) Condition 3: Maximum flux at the right external limb.

Using the same procedure applied in *Conditions 1* and *2*, only with the fact that the flux reaches its peak value in the right external limb (phase C), this in this case equation (6) is obtained.

$$3 \times N \times I_C = 2 \times \Re_{L1} \times \phi + \Re_{L2} \times \phi + 4 \times \Re_{Y1} \times \phi \\ + \Re_{Y2} \times \phi + \Re_e \times \frac{\phi}{2} + \Re_c \times \frac{\phi}{2} + 2 \times \Re_d \times \phi \quad (6)$$

The equation system as a function of the magnetization currents in each phase, fluxes and reluctances of limbs and yokes and for the air gaps in the core is them computed through the use of equations (4), (5) and (6). Solving the three equation system it is possible to acquire the values of air gap reluctances, as shown in equations (7), (8) and (9):

$$\Re_e = \frac{N}{3 \times \phi} \times (5 \times I_A - I_B - I_C) - \frac{1}{9} \times (6 \times \Re_{L1} + 3 \times \Re_{L2} + \\ + 16 \times \Re_{Y1} + 2 \times \Re_{Y2}) \quad (7)$$

$$\Re_c = \frac{N}{3 \times \phi} \times (-I_A + 5 \times I_B - I_C) - \frac{1}{9} \times (6 \times \Re_{L1} + 3 \times \Re_{L2} + \\ + 8 \times \Re_{Y1} - 8 \times \Re_{Y2}) \quad (8)$$

$$\Re_d = \frac{N}{3 \times \phi} \times (-I_A - I_B + 5 \times I_C) - \frac{1}{9} \times (6 \times \Re_{L1} + 3 \times \Re_{L2} + \\ + 16 \times \Re_{Y1} + 2 \times \Re_{Y2}) \quad (9)$$

4) Routine for the determination of magnetic material reluctance in the condition of flux peak value.

The magnetic flux and the magnetic induction can be computed respectively by equations (10) and (11).

$$\phi = \frac{V}{4.44 \times N \times f} \quad (10)$$

$$B = \frac{\phi}{A_m} \quad (11)$$

Where:

- V – Winding voltage rms value [V]
- ϕ – Magnetic flux (peak) [Wb];
- N – Turns number;
- F – Frequency [Hz];
- B – Magnetic induction [T];
- A_m – Transversal cross section area for the ferromagnetic core [m^2].

Once obtained the value of B, the magnetic field H can determined trough the material B against H curve. Thus, the permeability can be computed through equation (12):

$$\mu = \frac{B}{H} \tag{12}$$

where:

μ – Absolute magnetic permeability [H/m];
H – Magnetic field [A/m].

Equation (13) is used to estimate limb ($\Re_L$) and yoke ($\Re_Y$) reluctances.

$$\Re = \frac{l}{\mu \times A} \tag{13}$$

Where:

$\Re$ – $\Re_{L1}$, $\Re_{L2}$, $\Re_{Y1}$ or $\Re_{Y2}$ reluctances [H^{-1}];
l – Average length of limb or yoke [m];
A – Transversal section for the limb or yoke [m^2].

With the substitution of $\Re_{L1}$, $\Re_{L2}$, $\Re_{Y1}$ and $\Re_{Y2}$ in equations (7), (8) and (9), it is possible to obtain reluctances $\Re_e$, $\Re_c$ and $\Re_d$.

The air gap lengths can be estimated through expression (13) using the air permeability as $\mu_o = 4\pi 10^{-7}$H/m.

TABLE IV
VALUES OBTAINED FOR THE CALCULATION OF AIR GAP THICKNESS

Variable	Rating
ϕ	0.007223 Wb
μ_L (Bmáx)	0.0303 H/m
μ_L (Bmáx/2)	0.0388 H/m
μ_Y (Bmáx)	0.0366 H/m
μ_Y (Bmáx/2)	0.0385 H/m
$\Re_{L1}$	1,806.65 H^{-1}
$\Re_{L2}$	1,410.86 H^{-1}
$\Re_{Y1}$	887.43 H^{-1}
$\Re_{Y2}$	843.63 H^{-1}

C. *Air gap calculation*

The computation methodology was presented in the previous section, so, in this section will be shown only the values for each of the parameters used to estimate the thickness of each air gap. Table IV shows such figures.

Once determined the reactance of limbs and yokes for the two flux conditions, it will be possible to compute reluctances $\Re_e$, $\Re_c$ and $\Re_d$ through equations (7), (8) and (9), obtaining in this case:

$$\Re_e = 20{,}294.19 \ \ H^{-1}$$

$$\Re_c = 7{,}547.36 \ \ H^{-1}$$

$$\Re_d = 2{,}0294.19 \ \ H^{-1}$$

Using equation (13), and also the figures already known, the values of air gap thickness are obtained, as shown below.

$$l_e = l_d = 0.12mm$$

$$l_c = 0.045mm$$

As expected, the air gaps are very thin, almost insignificant, when compared with the length of limbs and yokes, due to this, they are generally neglected. However, reluctances of such air gaps can be larger than the reluctances of the magnetic parts; thus, the magnetomotive force required to establish the magnetic flux in the air gap is larger.

When implementing such air gaps in the transformer model in FEMM, Figure 7 is obtained after running a simulation. In this figure it is possible to note a reduction in the values of magnetic flux density. The flux density at the limb and yokes dropped respectively to 1.54 T and 1.46 T. Thus, it is a truth that the air gaps are important for the establishment of the real transformer core magnetization characteristic.

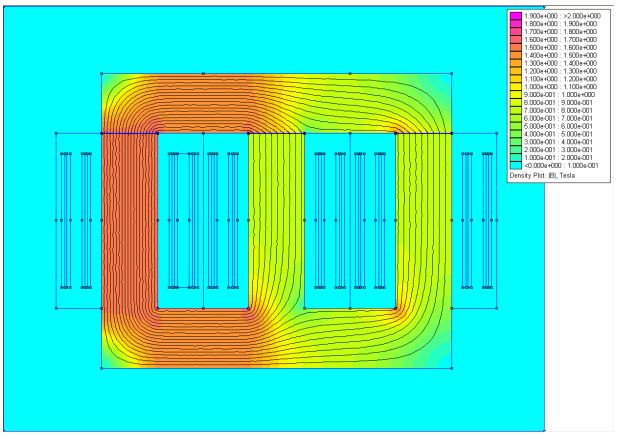

Fig. 7. Transformer simulation in FEMM with the insertion of air gaps.

Beyond the consideration for the current peak at phase A, simulations were made considering instants in which currents in phases B and C have their respective peak values. In all the simulated cases it was observed that the magnetic flux density for the limbs and yokes, for the maximum flux condition, where very close of expected values, 1.55 T and 1.44 T for limbs and yokes respectively.

D. *Calculation of leakage reactance*

Leakage reactance can be estimated using the same magnetic structure already incorporated at the FEMM program [1, 7]. The recommendation is to use the total energy stored in the volume of air represented by the core window around the coils, when it is applied the same magnetomotive force (mmf) in both windings (primary and secondary). In this situation the magnetization is negligible. Such energy can be obtained by the post-processing phase, considering the volume defined by the window area and the core depth [8]. In this case, the following adjustment should be made: divide the calculated energy by the core depth and multiply by the length of the average core window circunference. The leakage inductance can be calculated through the use of equation (14).

$$L = \frac{2 \times w}{I^2} \tag{14}$$

Where:

L – Leakage inductance [H];
w – Total energy stored in the air volume [J];
I – Winding current [A].

In the case under investigation, it was applied the rated current in each phase individually, in both windings. Table V shows the values for the leakage reactance found for each of the phases. Must be highlighted that the value obtained for the short-circuit test (load test) is 3.47%, and the average value obtained in the simulation with FEMM is 3.5345%, which gives us a percent difference of 0.065%.

TABLE V
PERCENT LEAKAGE REACTANCE OBTAINED THROUGH THE SIMULATION USING FEMM

X_A [%]	X_B [%]	X_C [%]
3.5341	3.5347	3.5348

IV. CONCLUSIONS

This work highlights the use of air gaps arising from the assembling procedures for the magnetic steel sheets in the composition of the transformer core. Such air gaps with the companion of the silicon steel sheet magnetization curve given by the manufacturer makes dispensable the setting up of the transformer magnetization, which some times is unworkable.

The air gaps reluctances and, consequently, their lengths, are estimated as a function of magnetic material reluctances for the limb and yokes and magnetization current peak values, which must be obtained from the no-load current waveform.

The core magnetic flux distribution in its various instants can be determined by imposing the current instantaneous values in the windings, which can be obtained through measurements or time domain simulations.

It is possible to verify through expressions (4), (5) and (6) that if the mentioned air gaps did not exist the magnetization current peak value will be approximately 15% of the measured value. The meaning is: the air gaps, although small, are responsible for the larger part of the magnetization current.

Once configured the transformer core and the average diameter of coils in the FEMM program, many variables can be found in the post-processing stage, such as the leakage reactance, mechanical stress due to magnetic generated forces in the windings and others. It is clear that for the leakage reactance a very close value to that measured in the short-circuit test was obtained.

ACKNOWLEDGMENTS

We would like to thank the monetary assistance from the Brazilian Ministry of Education by way of its grant agency CAPES – *Coordenação de Aperfeiçoamento de Pessoal de Nível Superior*, and the institutional support of Universidade Federal de Uberlândia, School of Electrical Engineering through its Electrical Systems Dynamics Group and Rural Electricity and Alternative Energy Sources Laboratory.

REFERENCES

[1] JAMALI, S.; ARDEBILI, M.; ABBASZADEH,K. - "Calculation of short-circuit reactance and electromagnetic forces in three-phase transformer by finite element method" *Proceedings of the Eighth International Conference on Publication Electrical Machines and Systems, 2005. (ICEMS 2005).* pgs: 1725- 1730 - Vol. 3.

[2] WATERS, M. - "The Short-Circuit Strength of Power Transformers" 5. ed. [S.l.]: *Macdonald & Co., London*, 1966.

[3] FUCHS, E.F.; YOU, Y. - "Measurement of λ-i Characteristics of Asymmetric Three-Phase Transformers and Their Applications" *IEEE Transactions on Power Delivery, Vol 17, Nº 4, October 2002*.

[4] HEATHCOTE, J. M. - "J and P Transformer Book" 12. ed. [S.l.]: *Elsevier Science Ltd, Oxford*, 1998.

[5] AZEVEDO, A.C.; REZENDE, I.; DELAIBA, A.C.; OLIVEIRA, J.C.; CARVALHO, B.C.; BRONZEADO, H.C. - "Investigation of Transformer Electromagnetic Forces Caused by External Faults Using FEM" *Transmission & Distribution Conference and Exposition: Latin America, 2006*. TDC´06. IEEE/PES, pgs:1-6.

[6] MEEKER, D. - "Finite Element Method Magnetic" - *Version 4.2 - User´s Manual, September 2006.*

[7] JAMALI, S.; ARDEBILI, M.; ABBASZADEH,K.; TOLIYAT, H.A. - "Winding Arrangement effects on Electromagnetic Forces and Short-Circuit Reactance Calculation in Power Transformers via Numerical and Analytical Methods" *Proceedings of the 12th Biennial IEEE Conference on Electromagnetic Field Computation* (CEFC 2006).

[8] KULKARNI, S.V.; KHAPARDE, S.A. - "Transformer Engineering - *Design and Practice"Marcel Dekker, Inc., 2004.*